BIOCHEMISTRY
including biophysical chemistry & molecular biology

Article

pubs.acs.org/biochemistry

Mutation of Trimethyllysine 72 to Alanine Enhances His79–Heme-Mediated Dynamics of Iso-1-cytochrome *c*

Melisa M. Cherney,[†] Carolyn C. Junior, and Bruce E. Bowler*

Department of Chemistry and Biochemistry, Center for Biomolecular Structure and Dynamics, University of Montana, Missoula, Montana 59812, United States

Supporting Information

ABSTRACT: Trimethyllysine 72 (Tml72) of yeast iso-1-cytochrome *c* lies across the surface of the heme crevice loop (Ω-loop D, residues 70–85) like a brace. Lys72 is oriented similarly in horse cytochrome *c* (Cyt*c*). To determine whether this residue affects the dynamics of opening the heme crevice loop, we have studied the effect of a Tml72 to Ala substitution on the formation of the His79–heme alkaline conformer near neutral pH using a variant of iso-1-Cyt*c* including K72A and K79H mutations. Guanidine hydrochloride denaturation shows that the Tml72 to Ala substitution within error does not affect the global stability of the protein. The effect of the Tml72 to Ala substitution on the thermodynamics of the His79–heme alkaline transition is also small. However, pH-jump kinetic studies of the His79–heme alkaline transition show that both the forward and backward rates of conformational change are increased by the Tml72 to Ala substitution. The barrier for opening the heme crevice is reduced by 0.5 kcal/mol and for closing the heme crevice by 0.3 kcal/mol. The ability of Tml72 to modulate the heme crevice dynamics may indicate a crucial role in regulating function, such as in the peroxidase activity seen in the early stages of apoptosis.

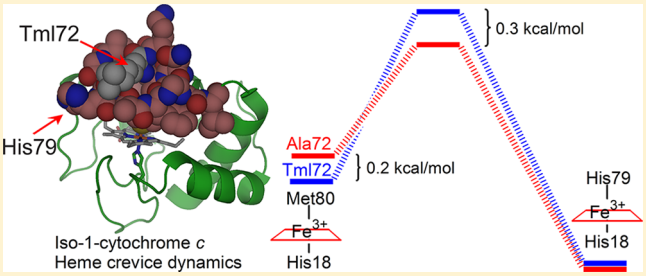

Small globular proteins fold to a single predominant structure generally accepted to be the most stable form of the protein under physiological conditions.[1,2] However, recent work indicates that less stable, albeit thermally accessible, conformations exist for many proteins.[3] Such alternate conformers are thought to be important for protein function. They can involve alternate side chain rotamers,[4] coordinated reorientation of side chains,[5,6] local changes in loop or secondary structure,[7] and large domain motions.[8]

Mitochondrial cytochrome *c* (Cyt*c*) is known to undergo rearrangements around the heme crevice loop (red loop in Figure 1) that are thought to be important for function. The best-studied of these rearrangements is the alkaline conformational transition,[9,10] which occurs at moderately alkaline pH and involves a replacement of the Met80 ligand in the sixth coordination site of the heme with either Lys73 or Lys79 from the heme crevice loop.[11] A nuclear magnetic resonance (NMR) structure of the Lys73 alkaline conformer shows that the heme crevice is significantly rearranged relative to that of the native conformer.[12] Lys79 being sequentially adjacent to Met80 is expected to cause less structural perturbation to Cyt*c* when it displaces Met80 to form the Lys79 alkaline conformer. Thermodynamic data are consistent with the Lys79 alkaline conformer causing a smaller perturbation to the structure of Cyt*c* than the Lys73 alkaline conformer.[11,13,14]

Besides its role in the electron transport chain, Cyt*c* also acts as an important signaling agent in the intrinsic pathway of apoptosis.[15] Initially, studies of the role of Cyt*c* in apoptosis focused on the binding of Cyt*c* to Apaf-1 to form the apoptosome, which triggers the caspase cascade.[16,17] Lys72 has an important effect on Apaf-1 binding, and in fact, the trimethylation of this residue in yeast iso-1-Cyt*c* was originally thought to render iso-1-Cyt*c* incapable of inducing the caspase

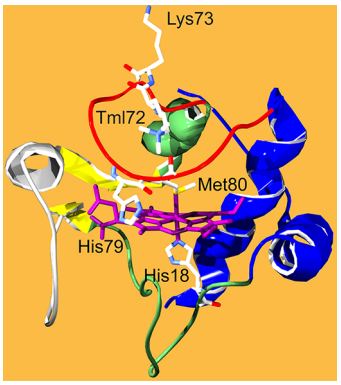

Figure 1. Structure of yeast iso-1-Cyt*c* showing the K79H mutation. Protein Data Bank entry 2ycc was used and the K79H mutation inserted in silico (Swiss-Pdb Viewer 4.0.4). The side chains of Lys73 and trimethyllysine 72 (Tml72) are shown as sticks. The heme (purple) and its native state ligands, His18 and Met80, are also shown. The heme crevice loop is colored red.

Received: November 28, 2012
Revised: January 10, 2013
Published: January 11, 2013

cascade.[18,19] Interestingly, trimethylation is sufficient to eliminate caspase-9 activation by horse Cyt*c*,[16,20] but a lack of trimethylation of iso-1-Cyt*c* is not sufficient for iso-1-Cyt*c* to be able to activate the caspase cascade.[20] Additional mutations on the surface of iso-1-Cyt*c* are required for it to be able to trigger the caspase cascade.[16]

More recently, it was shown that Cyt*c*-mediated oxidation of cardiolipin, an important mitochondrial matrix lipid, is an important step early in apoptosis that leads to the release of Cyt*c* into the cytoplasm.[21] The peroxidase activity needed to oxidize cardiolipin requires Cyt*c* to have an open heme coordination site. The interaction of Cyt*c* with cardiolipin leads to the loss of Met80−heme ligation[21,22] and may lead to population of alkaline conformers and conformers with H_2O or OH^- bound in the sixth coordination site of the heme near neutral pH.[23,24] There is also evidence that alkaline conformers may be involved early in apoptosis[25] when oxidation of cardiolipin by the peroxidase activity of Cyt*c* is important. However, it is clear that alkaline conformers, which block the sixth coordination site of the heme with a strong ligand, will not be competent for peroxidase activity.[26] Thus, it is important to understand the structural factors that can modulate formation of Cyt*c* conformers with a weaker ligand like H_2O or OH^- bound to the sixth coordination site of the heme, which is necessary for peroxidase activity.

Inspection of the structure of yeast iso-1-Cyt*c* shows that trimethyllysine 72 (Tml72) lies across the surface of the heme crevice loop (red in Figure 1) like a brace.[27] The methyl groups of Tml72 make close contacts with the carbonyls of Thr78 and Met80, as well as the side chain of Ala81. In horse Cyt*c*, a similar orientation is found for Lys72 with H-bonds from the ε-NH_2 to the carbonyls of Met80 and Phe82. Thus, in this work, we tested the hypothesis that the residue at position 72, beyond its importance for binding to Apaf-1, may also play an important role in the dynamics of opening the heme crevice loop and allowing H_2O or OH^- to displace Met80. As a model system for studying the effect of Tml72 on the dynamics of the heme crevice loop of yeast iso-1-Cyt*c*, we use the His79-mediated alkaline conformational transition. The modest conformational perturbation expected for the His79-mediated alkaline transition is likely to be similar to that required for Met80 to swing out of the heme crevice loop and allow water to bind. These studies were conducted with pseudo-wild-type, WT*, iso-1-Cyt*c* expressed in *Escherichia coli*,[28] which carries a K72A mutation. The Tml72A substitution eliminates the strutlike interactions of Tml72 with the heme crevice loop found in yeast-expressed iso-1-Cyt*c*.[27] Comparison of the dynamics of the His79-mediated alkaline transition of WT*K79H with our previous work on the dynamics of this conformational transition using the yeast-expressed K79H (yK79H) variant[29] shows that Tml72 slows heme crevice dynamics. Thus, the residue at this position could modulate the peroxidase activity of Cyt*c* implicated in the release of Cyt*c* from mitochondria.[21]

EXPERIMENTAL PROCEDURES

Preparation of the WT*K79H Variant of Iso-1-Cyt*c*. The WT*K79H variant of iso-1-Cyt*c* was prepared in the pRbs_BTR1 vector,[30] which is a derivative of the pBTR1 vector.[31] The pRbs_BTR1 vector contains an optimized ribosomal binding site[32] and like the pBTR1 vector co-expresses yeast heme lyase (*CYC3*), permitting covalent attachment of heme in the cytoplasm of *E. coli*.[28] The K79H mutation was introduced via polymerase chain reaction-based mutagenesis and the sequence confirmed by dideoxy sequencing at the Murdock DNA Sequencing Facility (University of Montana). The WT* background carries a C102S mutation to prevent dimerization during physical studies and a K72A mutation to prevent the formation of the Lys72−heme alkaline conformer.[28]

Growth and Purification of Iso-1-Cyt*c* Carrying the K79H Mutation. The WT*K79H variant was produced from *E. coli* BL21(DE3) cells (EdgeBio, Gaithersburg, MD) using methods described previously.[33] Briefly, cells freshly transformed with the pRbs_BTR1 vector carrying WT*K79H iso-1-Cyt*c* on an L-ampicillin plate were suspended in 3 mL of sterile L-broth and used to inoculate 1 L of 2×YT medium in a 2.8 L Fernbach flask. The cells were typically grown at 37 °C in a shaker incubator (125 rpm) for 18 h. Cells were harvested by centrifugation for 10 min at 4 °C and 5000 rpm (GS-3 rotor) with a Sorvall RC 5C+ centrifuge, and the bright pink cell pellet was stored at −80 °C until it was used. Prior to cell lysis, the cell pellet was subjected to two cycles of thawing (4 °C) and freezing (−80 °C). The cells were then thawed at 4 °C and resuspended in 2 mL of lysis buffer [50 mM Tris (pH 8), 500 mM NaCl, and 1 mM EDTA] per gram of cells. A few crystals of DNase I and RNase A were added, and the protease inhibitor, PMSF, was added to a final concentration of 2 mM. The cells were then lysed by at least three passes through a French pressure cell at a cell pressure of 16000 psi.

Purification procedures for iso-1-Cyt*c* variants have been described previously.[34,35] Briefly, cell lysates cleared by centrifugation for 30 min at 4 °C and 10000 rpm (GSA rotor) were brought to 50% ammonium sulfate saturation. After equilibration for at least 3 h at 4 °C (but usually overnight), precipitate was removed by centrifugation for 30 min at 4 °C and 10000 rpm (GSA rotor) and the supernatant dialyzed against two changes of 12.5 mM sodium phosphate buffer (pH 7.2), 1 mM EDTA, and 2 mM β-mercaptoethanol (β-ME). The dialyzed protein solution was then batch-adsorbed onto 100 mL of CM Sepharose Fast Flow resin equilibrated to 50 mM sodium phosphate buffer (pH 7.2), 1 mM EDTA, and 2 mM β-ME. The resin was then packed into a 2.5 cm × 20 cm glass column, and a 200 mL linear gradient from 0 to 0.8 M NaCl in 50 mM sodium phosphate buffer (pH 7.2), 1 mM EDTA, and 2 mM β-ME was used to elute the protein. Eluent containing iso-1-Cyt*c* was concentrated by ultrafiltration, flash-frozen in liquid nitrogen, and stored at −80 °C in 1.5 mL aliquots containing 3−6 mg of protein.

Just before the experiments, protein was thawed and purified to homogeneity by high-performance liquid chromatography (Agilent 1200 series) using a Bio-Rad UNO S6 column. The following gradient at a flow rate of 3 mL/min was used: 0% B for 7 min, 0 to 30% B over 27 min, 30% B for 6 min, 30 to 100% B over 3 min, 100% B for 7 min, 100 to 0% B over 3 min, and 0% B for 10 min. Buffer A is 50 mM sodium phosphate (pH 7). Buffer B is 50 mM sodium phosphate (pH 7) and 1.0 M NaCl. Pure iso-1-Cyt*c* was concentrated and changed into 50 mM sodium phosphate (pH 7) by centrifuge ultrafiltration.

Immediately prior to each experiment, iso-1-Cyt*c* was oxidized with $K_3[Fe(CN)_6]$ as described previously.[29] The oxidized protein was separated from $K_3[Fe(CN)_6]$ by Sephadex G-25 size exclusion chromatography with the G-25 resin pre-equilibrated to buffer appropriate to the experiment.

Global Protein Stability Measured by Guanidine Hydrochloride Denaturation. Denaturation of the

WT*K79H variant by guanidine hydrochloride (GdnHCl) was monitored by circular dichroism (CD) using an Applied Photophysics Chirascan CD spectrometer equipped with a Hamilton MICROLAB 500 titrator. Titrations were conducted in the presence of 20 mM Tris (pH 7.5) and 40 mM NaCl at 25 °C using protocols described previously.[13] Ellipticity data were collected at 250 and 222 nm at each GdnHCl concentration, with θ_{250} used as background to correct for baseline drift during the titration. Plots of $\theta_{222} - \theta_{250}$ were fit by nonlinear least-squares methods to a two-state model assuming a linear dependence of the free energy of unfolding, ΔG_u, on GdnHCl concentration.[36] Cyt*c* typically shows curvature in the native baseline because of specific Cl^- binding at low GdnHCl concentrations.[37] To deal with this issue, points from the curved part of the native baseline are not included in the fit and the native state baseline is assumed to be independent of GdnHCl concentration.[38]

Local Protein Stability Measured by pH Titration at 695 nm. The alkaline conformational transition of the WT*K79H variant was monitored at 695 nm, a weak absorbance band sensitive to Met80−heme ligation.[39] Titrations were conducted at room temperature, 22 ± 1 °C, in 0.1 M NaCl, as described previously.[29,40] Briefly, 400 μL of oxidized protein in 0.2 M NaCl at ∼400 μM protein (2× protein stock) was mixed with 400 μL of deionized water to prepare the 0.1 M NaCl solution of ∼200 μM protein for the pH titration. The pH was adjusted to approximately 5 using equal volumes of 2× stock and a dilute HCl solution. The pH was recorded with a Denver Instruments UB 10 pH meter (Fisher Accumet semimicro calomel electrode, catalog no. 13-620-293). The absorbance spectrum was measured from 500 to 750 nm using a Beckman DU 800 UV−vis spectrometer. The iso-1-Cyt*c* concentration was evaluated at the starting pH of ∼5 using an ε_{570} of 5.2 mM^{-1} cm^{-1} and an ε_{580} of 3.5 mM^{-1} cm^{-1} [41] and ranged from 185 to 200 μM. The pH was increased in steps of ∼0.2 pH unit by adding equal volumes of 2× protein stock and dilute NaOH solution to the titration solution. The pH and the absorbance spectrum were measured after each addition of base. The absorbance at 750 nm, A_{750}, was used as background to correct for baseline variation during the titration. Plots of $A_{695} - A_{750}$ versus pH were fit to the thermodynamic model described in Results.[14]

pH-Jump Stopped-Flow Measurements. Oxidized WT*K79H iso-1-Cyt*c* was adjusted to ∼20 μM by dilution into 0.1 M NaCl. For upward pH-jump experiments, the 0.1 M solution of WT*K79H was adjusted to pH 5.05 (maximal population of the native state conformer). For downward pH-jump experiments, the 0.1 M NaCl solution of WT*K79H was adjusted to pH 7.99 (maximal population of His79−heme alkaline conformer). The protein solution was mixed in a 1:1 ratio with a 20 mM buffer containing 0.1 M NaCl to achieve the final desired pH using an Applied Photophysics (Leatherhead, U.K.) SX20 stopped-flow spectrometer. The temperature was kept at 25 °C with a Thermo Neslab RTE7 circulating water bath. The following 20 mM buffers were used: sodium acetate (pH 5.00 and 5.25), MES, sodium salt (pH 5.50, 5.75, 6.00, 6.25, and 6.50), monobasic sodium phosphate (pH 6.75, 7.00, 7.25, and 7.50), Tris (pH 7.75, 8.00, 8.25, 8.50, and 8.75), sodium borate (pH 9.00, 9.25, 9.50, 9.75, and 10.00) and CAPS, sodium salt (pH 10.25). The buffer pH was adjusted with HCl or NaOH solutions. After being mixed, the final solution consisted of ∼10 μM WT*K79H iso-1-Cyt*c*, 10 mM buffer, and 0.1 M NaCl. In general, data were collected at 406 nm on a 5 s time scale with pressure hold to follow millisecond time scale kinetics and on 100−300 s time scales to follow second time scale events. Data were fit to one to four exponential equations as appropriate.

RESULTS

Global Stability of the WT*K79H Variant. The WT*K79H variant of yeast iso-1-Cyt*c* is expressed in *E. coli*. The pseudo-wild-type, WT*, iso-1-Cyt*c* used to prepare the WT*K79H variant contains the C102S mutation used in protein expressed in *Saccharomyces cerevisiae* to prevent disulfide dimerization during physical studies. Lys72 is trimethylated for iso-1-Cyt*c* expressed in its native host, but not for protein expressed in *E. coli*.[28] When Lys72 is not trimethylated, a Lys72−heme conformer is a significant component of the alkaline state of iso-1-Cyt*c*.[28,42] Thus, WT* iso-1-Cyt*c* also contains a K72A mutation to prevent population of the Lys72−heme conformer. The K72A mutation also truncates the side chain at position 72 so that it can no longer act as a brace across the surface of the heme crevice loop (see Figure 1).

To ascertain whether the K72A mutation affects the global stability of the WT*K79H variant relative to the yK79H variant (Tml72), we have measured the global stability of this protein at pH 7.5 using GdnHCl denaturation methods (Figure 2). The

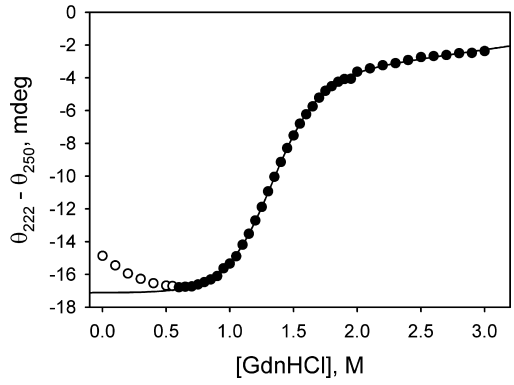

Figure 2. Plot of ellipticity vs GdnHCl concentration for the WT*K79H variant of iso-1-Cyt*c*. The filled black circles were used in fitting the data to a two-state model for protein unfolding assuming a linear dependence of the free energy of unfolding on GdnHCl concentration. The empty circles were excluded from the fit. The solid line is the fit of the data to a two-state model. Parameters from the fit are listed in Table 1.

thermodynamic parameters obtained from these data are compared to those of the yeast-expressed protein, yK79H, in Table 1. Clearly, the effect of alanine versus trimethyllysine at position 72 on global stability, $\Delta G_u^{\circ\prime}(H_2O)$, is modest. As with

Table 1. Thermodynamic Parameters from GdnHCl Denaturation of K79H Variants of Iso-1-Cyt*c* Expressed in *E. coli* versus Yeast at 25 °C

variant	$\Delta G_u^{\circ\prime}(H_2O)$ (kcal mol^{-1})	*m* (kcal mol^{-1} M^{-1})	C_m (M)
WT*K79H[a]	4.27 ± 0.11	3.27 ± 0.06	1.30 ± 0.02
yK79H[b]	4.45 ± 0.30	3.53 ± 0.25	1.26 ± 0.01

[a]Expressed in *E. coli*. Also, carries a K72A mutation. [b]Expressed in *S. cerevisiae*. Lys72 is trimethylated. Parameters from ref 29.

dx.doi.org/10.1021/bi301599g | *Biochemistry* 2013, 52, 837−846

the yeast-expressed protein, the GdnHCl *m*-value for WT*K79H iso-1-Cyt*c* is considerably smaller than the *m*-value of 4.5−5 kcal mol^{-1} M^{-1} observed for wild-type iso-1-Cyt*c* expressed in yeast.[38,43,44] The smaller *m*-value indicates that less surface area is exposed when K79H variants unfold,[45] which is consistent with this variant being primarily in the partially unfolded His79−heme alkaline conformer at pH 7.5 (see below and ref 29).

Thermodynamic and Kinetic Models for the His79−Heme Alkaline Transition of Iso-1-Cyt*c*. We have characterized a number of variants of iso-1-Cyt*c* that have one of the alkaline state ligands, Lys73 or Lys79, mutated to histidine.[10,13,14,29,40,46−54] The alkaline transition of wild-type iso-1-Cyt*c* shows a single phase when monitored with absorbance at the 695 nm band (A_{695}),[11,13,14,28] which reports on heme-Met80 ligation in oxidized Cyt*c*.[39] Typically, the pH dependence of A_{695} for the alkaline transition can be fit to the Henderson−Hasselbalch equation as a one-proton process with an apparent pK_a ranging from 7 to 11 for forms of cytochrome *c* from various sources.[39] When Lys79 or Lys73 of iso-1-Cyt*c* is replaced with histidine, a His−heme alkaline conformer is populated between pH 6 and 8 (Figure 3). The equilibrium

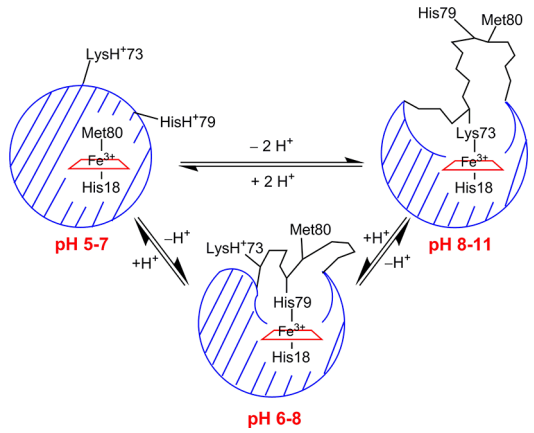

Figure 3. Thermodynamic model for the alkaline conformational transition of WT*K79H iso-1-Cyt*c*. Note that for the direct conversion of the native state to the Lys73−heme alkaline conformer only one of the two protons is thermodynamically linked to the conformational change. The second proton is due to ionization of His79.

constants for His73−heme and His79−heme alkaline conformers relative to the native state (Met80−heme) are typically near 1, so loss of Met80 ligation (decrease in A_{695}) is not complete near pH 7.5. Above pH 7.5, formation of the Lys−heme alkaline conformer, due to the remaining lysine (Lys73 or Lys79) in the heme crevice loop, drives the complete loss of heme-Met80 ligation. Thus, K73H and K79H variants of iso-1-Cyt*c* typically have biphasic alkaline conformational transitions when monitored at 695 nm.

In Figure 3, the His79−heme alkaline conformer forms at a lower pH. However, because the native conformer is not completely converted to the His79−heme alkaline conformer near pH 7.5, some of the Lys73−heme alkaline conformer forms directly from the native conformer and some from the His79−heme alkaline conformer. Our interest is in the stability of alkaline conformers relative to the native conformer. Thus, we analyze the thermodynamic scheme in terms of the equilibria between the native state and each of the alkaline conformers, yielding eqs 1 and 2 for the dependence of $A_{695} - A_{750}$ on pH

$$A_{695} - A_{750} = \frac{A_N + A_{alk}K_{obs}}{1 + K_{obs}} \quad (1)$$

$$K_{obs} = \frac{K_C(H79)}{1 + \frac{[H^+]}{K_{H79}}} + \frac{K_C(K73)}{1 + \frac{[H^+]}{K_{K73}}} = \frac{10^{-pK_C(H79)}}{1 + 10^{pK_{H79}-pH}} + \frac{10^{-pK_C(K73)}}{1 + 10^{pK_{K73}-pH}} \quad (2)$$

where A_N is $A_{695} - A_{750}$ for the native state and A_{alk} is $A_{695} - A_{750}$ for complete loss of heme-Met80 ligation. $K_C(H79)$ [$pK_C(H79)$] is the equilibrium constant for the conformational equilibrium between the native state and the His79−heme alkaline conformer when His79 is fully deprotonated, and $K_C(K73)$ [$pK_C(K73)$] is the equilibrium constant for the conformational equilibrium between the native state and the Lys73−heme alkaline conformer when Lys73 is fully deprotonated. K_{H79} (pK_{H79}) is the ionization constant of His79, and K_{K73} (pK_{K73}) is the ionization constant of the group that triggers formation of the Lys73−heme conformer. On the basis of recent studies of a series of Lys → Ala variants in the heme crevice loop (residues 70−85) of iso-1-Cyt*c*, we assume that pK_{K73} is the pK_a for Lys73 and set pK_{K73} equal to 10.8[42] in fitting $A_{695} - A_{750}$ versus pH to eqs 1 and 2.

The standard model for the kinetics of the alkaline conformational transition of Cyt*c* involving Lys−heme alkaline conformers[55] comprises a rapid deprotonation equilibrium (usually designated K_H or pK_H) followed by a conformational change with forward and backward rate constants, k_f and k_b, respectively, as shown in Figure 4A. In this model, the pH dependence of the observed rate constant, k_{obs}, and amplitude, ΔA, are described by eqs 3 and 4.

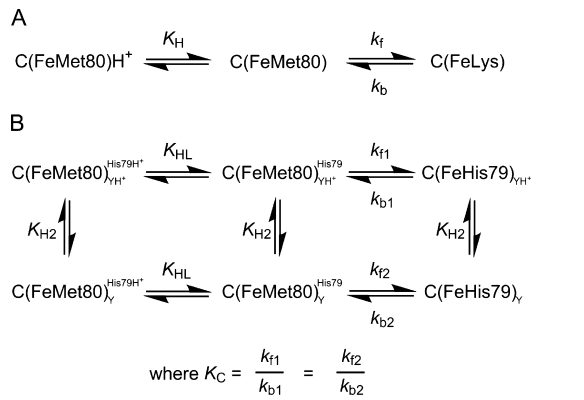

Figure 4. (A) Standard kinetic mechanism for the Lys−heme alkaline conformational transition. (B) Kinetic mechanism for the His79−heme alkaline transition. In both schemes, C(FeMet80) represents the native state of Cyt*c*. For the sake of simplicity, protons released in acid dissociation equilibria are not shown explicitly. In part A, C(FeLys) is a Lys−heme alkaline conformer. In part B, C(FeHis79) is the His79−heme alkaline conformer. The protonation state of His79 is indicated as a superscript for the native state of Cyt*c*. The subscripted YH^+ and Y represent the protonated and deprotonated forms, respectively, of an ionizable group that affects the dynamics of the alkaline transition. Acid dissociation constants and rate constants are defined in the text.

$$k_{obs} = k_b + k_f\left(\frac{1}{1 + 10^{pK_H - pH}}\right) \quad (3)$$

$$\Delta A = \Delta A_t\left[\frac{1}{1 + \frac{k_b}{k_f}(1 + 10^{pK_H - pH})}\right] \quad (4)$$

In eq 4, ΔA_t is the total amplitude for the alkaline transition. A number of protein groups, including the Lys ligand, Tyr67, heme propionates, His18, and a buried water molecule, have been considered as possible sources of the deprotonation that triggers the Lys−heme alkaline transition.[10,11,39]

We have shown that when the alkaline transition involves formation of His−heme conformers up to three deprotonation equilibria are required to explain the kinetics.[29,40,51] In the case of the His79−heme alkaline conformer, two ionizable groups are necessary to explain the kinetics of the alkaline transition.[29] The kinetic scheme used for the His79−heme alkaline transition is outlined in Figure 4B. As with the standard model for the alkaline transition, a rapid deprotonation equilibrium (K_{HL} or pK_{HL}) is followed by a conformational change. We find that pK_{HL} is near 6.5 for K79H and K73H variants of iso-1-Cyt*c*, indicating that the deprotonation equilibrium involves the histidine ligand that replaces Met80.[29,40,51] The ionization of the other ionizable group, $YH^+ \rightarrow Y$, affects the activation free energy for the conformational change. Thus, ionization of this group with K_{H2} (pK_{H2}) changes the magnitude of the forward and backward rate constants from k_{f1} and k_{b1} to k_{f2} and k_{b2}. In this model, the pH dependence of the observed rate constant, k_{obs}, and amplitude, ΔA, are described by eqs 5 and 6.[29,51]

$$k_{obs} = \left(\frac{K_{HL}}{K_{HL} + [H^+]}\right)\left(\frac{k_{f1}[H^+] + k_{f2}K_{H2}}{K_{H2} + [H^+]}\right) + \left(\frac{k_{b1}[H^+] + k_{b2}K_{H2}}{K_{H2} + [H^+]}\right) \quad (5)$$

$$\Delta A = \Delta A_t\left[\frac{1}{1 + \left(\frac{k_{b1}[H^+] + k_{b2}K_{H2}}{k_{f1}[H^+] + k_{f2}K_{H2}}\right)\left(1 + \frac{[H^+]}{K_{HL}}\right)}\right] \quad (6)$$

The kinetics of His−heme alkaline transition occur on a 0.1−1 s time scale, whereas the kinetics of the Lys−heme alkaline transition occur on a 10−100 s time scale[11,29,40,51,56] (see also Figures S2 and S3 of the Supporting Information). Thus, the rate constants and amplitudes are readily separable in time, and the kinetic data for the His79−heme alkaline transition and the Lys73−heme alkaline transition for WT*K79H iso-1-Cyt*c* can be fit independently to the kinetic models in panels B and A of Figure 4, respectively.

Equilibrium Studies of the Alkaline Conformational Transition of WT*K79H Iso-1-Cyt*c*. The alkaline conformational transition of the WT*K79H variant was followed by absorbance at 695 nm, A_{695}, an absorbance band that is present in the oxidized form of Cyt*c* when the native Met80−heme bond is present.[39] A_{695} is highest near pH 5 where the native conformer is maximally populated (Figure 5). Above pH 5.5, A_{695} decreases, reaching a plateau from pH 7 to 8.5. Above pH 8.5, A_{695} decreases further. This biphasic behavior is consistent with a His79−heme alkaline conformer forming between pH 5.5 and 7 and being the dominant conformer between pH 7 and 8.5. Above pH 8.5, the His79−heme alkaline conformer is replaced with the Lys73−heme conformer (see the scheme in Figure 3). A single isosbestic point is observed near 610 nm between pH 5 and 7 (Figure S1 of the Supporting Information). Similarly, a single isosbestic point near 635 nm is observed between pH 8 and 10 (Figure S1 of the Supporting Information). These isosbestic points are consistent with our previous work on the yK79H variant.[29] Thus, to a first approximation, each step of the alkaline transition represents a two-state conformational change.

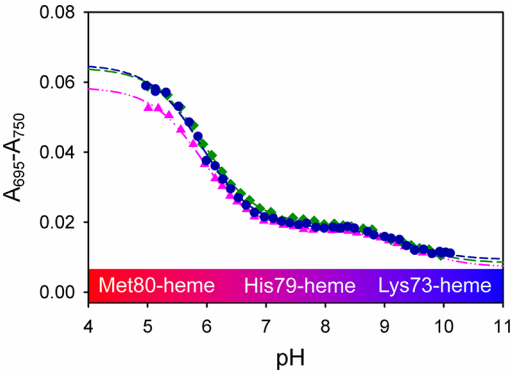

Figure 5. Plot of absorbance at 695 nm (background-corrected at 750 nm), $A_{695} - A_{750}$, vs pH for WT*K79H iso-1-Cyt*c*. Data from three independent runs are shown. The dashed lines are fits to eqs 1 and 2, assuming the protein is fully native near pH 5. Parameters from the fit are listed in Table 2.

In our previous work on the yK79H variant, we showed that the extinction coefficient at 695 nm, ε_{695}, for wild-type (WT) yeast-expressed iso-1-Cyt*c* was considerably higher than that of the yK79H variant at pH 5, suggesting that the yK79H variant may not be fully native at this pH. However, this observation is ambiguous because there is evidence that the heme−Met80 bond can exist in the oxidized state of Cyt*c* without significant absorbance at 695 nm.[31,57,58] Thus, ε_{695} may be sensitive to the local environment around the heme.[59,60]

For the sake of simplicity, the A_{695} versus pH data for the WT*K79H variant in Figure 5 have been fit to the thermodynamic model in Figure 3 (eqs 1 and 2), assuming that the protein is fully native near pH 5. Table 2 compares the thermodynamic parameters obtained for the alkaline transition of the WT*K79H variant to those obtained from A_{695} versus pH data for yK79H iso-1-Cyt*c* obtained with the same assumption.[29] The stability of the His79−heme alkaline conformer relative to the native state, pK_C(H79), does not depend on whether position 72 is Ala versus Tml. The pK_a of His79, pK_{H79}, of ∼6.7 extracted from the fit is in the range expected for a surface-exposed histidine,[61] consistent with the assignment of His79 as the ligand replacing Met80 between pH 6 and 8. Only the stability of the Lys73−heme alkaline

Table 2. Thermodynamic Parameters for the Formation of Alkaline Conformers of K79H Variants of Iso-1-Cyt*c* in 0.1 M NaCl at 22 ± 1 °C

variant	pK_C(H79)	pK_{H79}	pK_C(K73)[a]
WT*K79H	−0.61 ± 0.07	6.64 ± 0.05	−2.1 ± 0.2
yK79H[b]	−0.63 ± 0.08	6.71 ± 0.07	−2.9 ± 0.2

[a]In fits to eqs 1 and 2, pK_{K73} was set to 10.8 based on ref 42. [b]Parameters from Table 1 of ref 29.

dx.doi.org/10.1021/bi301599g | *Biochemistry* 2013, 52, 837−846

conformer relative to the native conformer, pK_C(K73), is significantly affected by changing Tml72 to Ala (Table 2).

pH-Jump Kinetics of the Alkaline Conformational Transition of WT*K79H Iso-1-Cytc. We determined the dynamics of the alkaline conformational transition of WT*K79H iso-1-Cyt*c* using pH-jump kinetic methods. Depending on the ending pH, two to four phases were observed in upward pH-jump experiments from pH 5 where the native state of the protein is maximally populated (Tables S1−S4 and Figure S2 of the Supporting Information). In our previous work on yK79H iso-1-Cyt*c*,[29] we observed only two phases. This difference may reflect the effect of Tml72 on the dynamics of the heme crevice loop (residues 70−85), but it may also reflect the lower signal-to-noise ratio of our previous data set.

The fastest phase, with a rate constant $k_{obs,1}$ from 200 to 450 s^{-1} (Table S1 of the Supporting Information) is only observed reliably above pH 8. This fast phase may represent a transient intermediate formed at higher pH. By pH 10, the $k_{obs,1}$ phase accounts for approximately one-third of the total amplitude. We also observe a low-amplitude phase with rate constant, $k_{obs,3}$, near 1 s^{-1} (Table S3 of the Supporting Information). A similar time scale low-amplitude phase is seen in conformationally gated electron transfer studies of the dynamics of the heme crevice loop of iso-1-Cyt*c* variants carrying a K73H mutation.[46,47] We have speculated that this phase may be due to a conformational change involving the acid state of iso-1-Cyt*c* in the low-pH regime and a conformational change involving a high-spin species at alkaline pH.[46,47] With the K73H variants, we observed this phase from pH 5 to 9.5 in our conformationally gated electron transfer studies. However, $k_{obs,3}$ is observed only above pH 7.3 with the WT*K79H variant. Below pH 7.3, it is likely that $k_{obs,2}$ and $k_{obs,3}$ would become indistinguishable for the WT*K79H variant, if the magnitude of $k_{obs,3}$ for WT*K79H iso-1-Cyt*c* behaves in the same manner that was observed for the K73H variants below pH 7.3.[46,47] We focus on the properties of the two remaining phases that report on the dynamics of the interconversion between the native state and the His79−heme and Lys73−heme alkaline conformers apparent in the equilibrium titration in Figure 5.

Figure 6 shows the pH dependence of the rate constant, $k_{obs,2}$, corresponding to the formation of the His79−heme alkaline conformer of iso-1-Cyt*c*. $k_{obs,2}$ for WT*K79H iso-1-Cyt*c* increases with increasing pH from pH 5 to 8 and then subsequently decreases between pH 8 and 10. The magnitude of $k_{obs,2}$ at pH 8 is approximately double that for yK79H iso-1-Cyt*c* (Figure 6). However, $k_{obs,2}$ decreases to smaller values at pH 10 for WT*K79H iso-1-Cyt*c* than for yK79H iso-1-Cyt*c*.

A fit of the data in Figure 6 to the kinetic mechanism in Figure 4B (eq 5) gives a pK_{HL} near 6.8 and a pK_{H2} near 9, consistent with our previous work on the His79−heme alkaline transition of yK79H (Table 3). The pK_{HL} of ∼6.8 is similar to the pK_{H79} of ∼6.6 obtained from equilibrium data (Table 2), indicating that His79 acts as the triggering ionization for formation of the His79−heme conformer from the native state of WT*K79H iso-1-Cyt*c*. A pK_{H2} of ∼9 has been observed in the kinetics of formation of both His73−heme variants, with[47,51] and without[40] Lys79 present, and for yK79H iso-1-Cyt*c* (Table 3 and ref 29). Thus, this ionization appears to be a general modulator of heme crevice dynamics in the alkaline pH regime. We note that ionizable groups with pK_a values near 9 have been observed in the equilibrium alkaline transition of horse heart Cyt*c* using infrared spectroscopy[62] and circular dichroism spectroscopy at 695 nm.[63] The ionizable group responsible for pK_{H2} may be the same group mediating formation of the intermediate conformer observed in the alkaline transition in these studies.

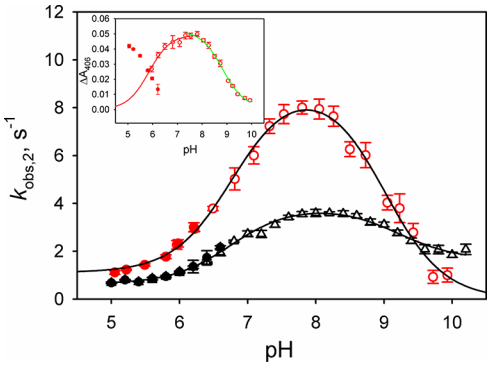

Figure 6. k_{obs} and amplitude at 406 nm, ΔA_{406}, vs pH from pH-jump experiments with WT*K79H iso-1-Cyt*c* for the His79−heme ($k_{obs,2}$) alkaline conformational transition at 25 °C in 0.1 M NaCl. The ΔA_{406} vs pH data are shown in the inset, and the $k_{obs,2}$ vs pH data are shown in the main panel. Empty red circles are from upward pH-jump experiments with a starting pH of 5.05, and filled red circles are from downward pH-jumps with a starting pH of 7.99. The empty (upward pH jumps) and filled (downward pH jumps) black triangles are pH-jump data for the His79−heme alkaline transition of yK79H iso-1-Cyt*c* taken from ref 29. The solid curves in the main panel are fits to eq 5. In the inset, the solid red line is a fit of the data from pH 6 to 7.8 to eq 4 with k_f and k_b set to the values of k_{f1} and k_{b1}, respectively, obtained from the fit of $k_{obs,2}$ vs pH to eq 5. The solid green curve in the inset is a fit of the data from pH 8 to 10 to the Henderson−Hasselbalch equation to yield pK_{H2}. The parameters from the fits to the data are listed in Table 3.

Table 3. Comparison of Rate and Ionization Constants for the His79−Heme Alkaline Transition of K79H Variants of Iso-1-Cyt*c* at 25 °C

parameter	WT*K79H[a]	yK79H[b]
k_{f1} (s^{-1})	8.0 ± 0.3	3.3 ± 0.2
k_{b1} (s^{-1})	1.1 ± 0.1	0.7 ± 0.2
k_{f2} (s^{-1})	0.0 ± 0.3	0.7 ± 0.1
k_{b2} (s^{-1})	∼0[c]	1.1 ± 0.1
pK_{HL} (k_{obs} data)	6.79 ± 0.06	6.75 ± 0.04
pK_{HL} (ΔA_{406} data)	6.76 ± 0.05[d]	6.8 ± 0.2
pK_{H2} (k_{obs} data)	9.00 ± 0.07	9.21 ± 0.02
pK_{H2} (ΔA_{406} data)	8.82 ± 0.05[e]	8.64 ± 0.02

[a]Errors are the standard errors from the fits to the data in Figure 6 reported by SigmaPlot 7. [b]Parameters for yK79H are from ref 29. [c]In fitting the k_{obs} vs pH data to eq 5, we made the simplifying assumption that the equilibrium constant for the formation of the His79−heme alkaline conformer from the native state is unaffected by pK_{H2} (see Figure 4B). This assumption allows us to reduce the number of variables in the fit by constraining k_{b2} with the equation $k_{b2} = k_{f2}(k_{b1}/k_{f1})$. [d]The p$K_{HL}$ from amplitude data was obtained by fitting the data from pH 6 to 7.8 to eq 4. [e]The pK_{H2} from amplitude data is from a fit of the amplitude data from pH 8 to 10 to the Henderson−Hasselbalch equation.

From pH 6 to 8, where k_{f1} and k_{b1} are dominant, both k_{f1} and k_{b1} are larger for WT*K79H iso-1-Cyt*c* than for yK79H iso-1-Cyt*c* (Figure 6 and Table 3). Thus, it appears that the Tml72 to Ala substitution lowers the activation barrier between the native state and the His79−heme conformer. The ionizable group corresponding to pK_{H2} slows the dynamics of interconversion

between the native state and the His79−heme conformer for both proteins. In the case of the yK79H variant, the native state/His79−heme alkaline conformational equilibrium shifts back toward the native state as a result of the pK_{H2} ionization (Table 3 and ref 29). The effect of the pK_{H2} ionization is much more pronounced for WT*K79H iso-1-Cyt*c*. The fit to eq 5 indicates that both k_{f2} and k_{b2} are zero within error.

The amplitude for formation of the His79−heme conformer of WT*K79H iso-1-Cyt*c* also increases up to pH 8 and then decreases, approaching zero above pH 10 (Figure 6, inset). Typically, fits to the pH dependence of the amplitude using eq 6 are constrained by the rate constants obtained from fits of the pH dependence of k_{obs} with eq 5.[29] Because both k_{f2} and k_{b2} are ∼0, eq 6 cannot be fit to the data in the inset of Figure 6 with well-defined constraints. Thus, we fit the amplitude data from pH 5 to 7.8 and from pH 8 to 10 separately. For the data from pH 5 to 7.8, we fit the amplitude data to the standard model for the alkaline conformational transition (eq 4),[55] using the values of k_{f1} and k_{b1} in Table 3 as constraints. The value of pK_{HL} obtained is consistent with that obtained from the k_{obs} versus pH data (Table 3). We fit the amplitude data from pH 8 to 10 to the Henderson−Hasselbalch equation, providing an estimate for pK_{H2} of 8.8. Thus, the ionizable group with the pK_a corresponding to pK_{H2} appears to be responsible for the decrease in the amplitude of this phase. Because a rapid competing process ($k_{obs,1}$) contributes strongly to the heme dynamics above pH 8, the loss of amplitude for the His79−heme phase may be primarily due to this competing process and thus does not provide reliable information about changes in the position of the native state/His79−heme alkaline state equilibrium because of ionization of the group corresponding to pK_{H2}.

Figure 7 shows data for the pH dependence of $k_{obs,4}$. The growth in the amplitude of this phase occurs over a pH range that is consistent with formation of the Lys73−heme alkaline conformer (Figure 7, inset). For the kinetics of formation of the Lys73−heme alkaline conformer, we use the standard kinetic model for the alkaline transition,[55] which involves a rapid deprotonation equilibrium of a single group preceding the conformational change (Figure 4A).

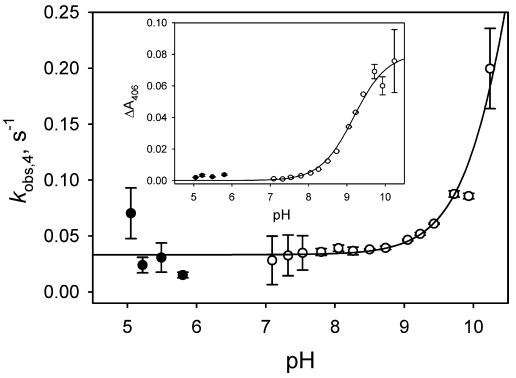

Figure 7. k_{obs} and amplitude at 406 nm, ΔA_{406}, vs pH data from pH-jump experiments with WT*K79H iso-1-Cyt*c* for the Lys73−heme ($k_{obs,4}$) alkaline conformational transition at 25 °C in 0.1 M NaCl. The ΔA_{406} vs pH data are shown in the inset, and the $k_{obs,4}$ vs pH data are shown in the main panel. Empty circles are from upward pH-jump experiments with a starting pH of 5.05, and filled circles are from downward pH jumps with a starting pH of 7.99. In the main panel, the solid curve is a fit to eq 3 with pK_H set to 10.8[42] as discussed in the text. In the inset, the solid curve is a fit to eq 4 with pK_H set to 10.8 and k_b set to the value obtained from the fit of eq 3 to the $k_{obs,4}$ vs pH data. Parameters from these fits are reported in the text.

Because the $k_{obs,4}$ versus pH data do not reach an upper limit, it is not possible to obtain a unique fit to eq 3. Therefore, we have set pK_H equal to 10.8, as an estimate for the pK_a of Lys73,[42] with the assumption that ionization of this group triggers the Lys73−heme alkaline transition. There is some evidence that deprotonation of lysine triggers formation of lysine−heme alkaline conformers.[42] However, the nature of the triggering ionization remains an unsettled issue.[9,10,39] The fit of the $k_{obs,4}$ versus pH data to eq 3 with a pK_H of 10.8 yields a k_b of 0.033 ± 0.004 s^{-1} and a k_f of 0.70 ± 0.06 s^{-1}. When the amplitude data in the inset of Figure 7 are fit to eq 4 with a k_b of 0.033 and a pK_H of 10.8, we obtain a k_f of 1.3 ± 0.2 s^{-1}. The magnitude of k_f obtained from these fits should be viewed with caution as it depends on the choice of pK_H. For the yK79H variant, the k_b of 0.037 ± 0.001 is very similar to that observed here for the WT*K79H variant. We observed a leveling off of k_{obs} for this phase above pH 10 with yK79H iso-1-Cyt*c*, which allowed an unconstrained fit to eq 3. The fit yielded a k_f of 0.23 ± 0.03 and a pK_H of 9.6 ± 0.2. The fit of the amplitude data to eq 4 (constrained with k_f and k_b from the fit to eq 3) for formation of the Lys73−heme alkaline conformer gave a pK_H of 9.44 ± 0.06. Thus, k_f is likely similar in magnitude for the yK79H and WT*K79H variants.

DISCUSSION

Effect of Tml72 on the Global Stability of Iso-1-Cyt*c*. The global stability of yK79H and WT*K79H iso-1-Cyt*c* are within error the same (Table 1). At first glance, this result is somewhat surprising given that Tml72 lies across the surface of the heme crevice loop. Thus, contacts that stabilize the native state are expected to be lost when Tml72 is substituted with Ala72 in the WT*K79H variant. However, as noted in Results, the *m*-values for the yK79H and WT*K79H variants of iso-1-Cyt*c* are ∼30% lower than for wild-type iso-1-Cyt*c*. The data in Figure 5 also show that the WT*K79H variant is predominately in the His79−heme conformer at pH 7.5 where global stability was measured. Thus, global unfolding monitored by CD spectroscopy is measuring unfolding from the His79−heme alkaline conformer. The similarity of the GdnHCl denaturation parameters for the yK79H and WT*K79H variants shows that the residue at position 72 does not contribute, within error, to the $\Delta G_u^{\circ\prime}(H_2O)$ of the His79−heme alkaline conformer relative to the GdnHCl denatured state.

Effect of Tml72 on the Stability the Native State Relative to Alkaline Conformers of Iso-1-Cyt*c*. Before we evaluate the effect of Tml72 on the stability of the native state relative to the His79−heme and Lys73−heme conformers, it is important to address the assumption that WT*K79H iso-1-Cyt*c* is fully native near pH 5, which was used in deriving the thermodynamic parameters for the alkaline conformational transition in Table 2. The k_{f1}/k_{b1} ratio of ∼8 for WT*K79H in Table 3 is consistent with pK_C(H79) being approximately −0.9 rather than approximately −0.6 (Table 2), as was determined with the assumption that WT*K79H is fully native at pH 5. If we assume that A_{695} at pH 8 corresponds to ∼$^1/_9$ {1/[1 + K_C(H79)], where K_C(H79) = k_{f1}/k_{b1}} of WT*K79H iso-1-Cyt*c* having Met80 bound to the heme and use this as a basis to evaluate A_N in eq 1, A_{695} for WT*K79H iso-1-Cyt*c* at pH 5 is actually consistent with only ∼60% of the protein being in the Met80-bound state. This estimate for the population of the native state at pH 5 is an upper limit because the fit of the data

dx.doi.org/10.1021/bi301599g | *Biochemistry* 2013, 52, 837−846

in Figure 6 to the kinetic model in Figure 4B assumes that WT*K79H iso-1-Cyt*c* is fully native at low pH and thus overestimates k_{b1}, leading to an underestimate of K_C(H73).

The k_{f1}/k_{b1} ratio of ∼5 for yK79H (Table 3) indicates that Tml72 does have a small stabilizing effect on the native state relative to the His79−heme alkaline conformer. Given that global unfolding monitored by CD proceeds from the His79−heme alkaline conformer, and the $\Delta G_u^{\circ\prime}(H_2O)$ values are within error identical for the WT*K79H and yK79H variants (Table 1), the stability of the His79−heme alkaline conformer relative to the denatured state appears to be unaffected by the Tml72 to Ala substitution. Thus, the stabilization of the native state relative to the His79−heme alkaline conformer is best attributed to interactions that Tml72 makes with the heme crevice loop in the native state that are not possible with Ala72.

In contrast to the His79−heme alkaline conformer, the Lys73−heme alkaline conformer is destabilized relative to the native state by the Tml72 to Ala substitution. The destabilization is also much more significant. From the difference between the pK_C(K73) for the WT*K79H variant and the yK79H variant in Table 2, the destabilization of the Lys73−heme alkaline state relative to the native state by the Tml72 to Ala substitution is 1.1 ± 0.4 kcal/mol at 22 ± 1 °C. The NMR structure of the Lys73−heme alkaline conformer of iso-1-Cyt*c* was conducted with Ala at position 72.[12] The structure shows that Ala72 is near the surface of the protein adjacent to the Met80 and Tyr67 side chains. The small side chain of Ala72 makes minimal contacts with Met80 and Tyr67. Interestingly, the aromatic cage motif that typically binds trimethyllysine in histones often contains both Met and Tyr residues.[64,65] Thus, Tml72 could participate in stabilizing interactions with Tyr67 (cation−π) and Met80 in the Lys73 alkaline conformer that would be eliminated by the Tml72 to Ala substitution, possibly leading to the observed 1.1 kcal/mol destabilization of the Lys73−heme alkaline conformer relative to the native state.

Tml72 Slows the Dynamics of the His79−Heme Alkaline Transition. The substitution of Tml72 with Ala leads to a 2.4-fold increase in k_{f1} and a 1.6-fold increase in k_{b1} for the interconversion between the native state and the His79−heme alkaline state. Thus, the barrier for this conformational transition is lowered in both directions by the Tml72 → Ala substitution. If we assume that the free energy of the His79−heme alkaline conformer is unaffected by the Tml72 → Ala substitution, as indicated by our global unfolding data, the increase in k_{b1} for WT*K79H iso-1-Cyt*c* relative to that of yK79H iso-1-Cyt*c* corresponds to a stabilization of the TS for the His79−heme alkaline transition by ∼0.3 kcal/mol at 25 °C for WT*K79H iso-1-Cyt*c* relative yK79H iso-1-Cyt*c*. The increase in k_{f1} for WT*K79H relative to that of yK79H corresponds to a reduction in the activation free energy for formation the His79−heme alkaline conformer by ∼0.5 kcal/mol at 25 °C. The 0.5 kcal/mol reduction in the barrier for formation of the His79−heme alkaline conformer from the native state would require an ∼0.2 kcal/mol destabilization of the heme crevice loop in the native state by the Tml72 → Ala substitution in addition to the ∼0.3 kcal/mol stabilization of the TS.

With regard to the possible impact of the residue at position 72 on the peroxidase activity for Cyt*c*, it is clear that Tml72 in wild-type iso-1-Cyt*c* slows the dynamics of heme crevice opening relative to Ala72, which would be expected to decrease peroxidase activity. Given that Lys72 in horse Cyt*c* also lies across the surface of the heme crevice loop and makes hydrogen bond contacts with main chain carbonyls of the heme crevice loop at Met80 and Phe82, a similar effect for Lys72 seems possible. Thus, our results suggest that the heme crevice loop has evolved to minimize undesirable peroxidase activity. The magnitude of the effect of a Tml72 → Ala substitution on peroxidase activity will depend on the details of the binding of oxygen species to the heme. If binding of oxygen species is fast relative to k_b (closing of the heme crevice), then binding of oxygen species and peroxidase activity will depend on the rate of opening of the heme crevice. However, if k_b is fast relative to binding of oxygen species, then peroxidase activity is controlled by an unfavorable equilibrium, opening of the heme crevice. For the Tml72 → Ala substitution, at least for the His79−heme alkaline transition we are using to model opening of the heme crevice, the maximal impact would be under conditions where binding of oxygen species is fast relative to closing of the heme crevice because the increase in k_{f1} is much larger than the net effect of the Tml72 → Ala substitution on the equilibrium.

Interestingly, the concentration of reactive oxygen species is expected to increase at the onset of apoptosis.[21] Under these conditions, the rate of heme crevice opening rather that the unfavorable equilibrium for heme crevice opening is likely to become more important for peroxidase activity. Thus, the residue at position 72 might play a role in setting the switch point (required level of reactive oxygen species) for turning on the peroxidase activity of Cyt*c* bound to cardiolipin at the onset of apoptosis.

■ CONCLUSION

In yeast iso-1-Cyt*c*, Tml72 lies across the surface of the heme crevice loop like a brace. A similar disposition of Lys72 is observed in horse Cyt*c*. We have shown that truncating this residue to an Ala increases heme crevice dynamics as modeled by the His79−heme alkaline transition. Our results suggest a possible role for the residue at position 72 in regulating the ease of heme crevice opening and the concomitant loss of Met80 ligation needed for Cyt*c* to gain the peroxidase activity required for oxidation of cardiolipin early in apoptosis.

■ ASSOCIATED CONTENT

Supporting Information

Tables containing rate constants and amplitudes from pH-jump kinetic studies and figures showing absorbance spectra as a function of pH and typical pH-jump kinetic data. This material is available free of charge via the Internet at http://pubs.acs.org.

■ AUTHOR INFORMATION

Corresponding Author

*Telephone: (406) 243-6114. Fax: (406) 243-4227. E-mail: bruce.bowler@umontana.edu.

Present Address

[†]Department of Chemistry and Biochemistry, University of Northern Iowa, Cedar Falls, IA 50614.

Funding

This research was supported by National Science Foundation Grant CHE-0910166.

Notes

The authors declare no competing financial interest.

■ ABBREVIATIONS

Cyt*c*, cytochrome *c*; Tml, trimethyllysine; *β*-ME, *β*-mercaptoethanol; GdnHCl, guanidine hydrochloride; $\Delta G_u^{\circ\prime}(H_2O)$, free energy of unfolding in the absence of denaturant; *m*-value, slope of a plot of free energy of unfolding versus denaturant concentration; WT*, pseudo-wild-type iso-1-cytochrome *c* expressed in *E. coli* carrying the C102S and K72A mutations. Mutations in protein variants are abbreviated by the one-letter code for the wild-type amino acid followed by the position number and then the one-letter code for the amino acid replacing the wild-type amino acid. For example, when Lys79 is replaced with His, it is designated K79H.

■ REFERENCES

(1) Haber, E., and Anfinsen, C. B. (1962) Side-chain interactions governing the pairing of half-cystine residues in ribonuclease. *J. Biol. Chem. 237*, 1839−1844.

(2) Anfinsen, C. B. (1973) Principles that govern the folding of protein chains. *Science 181*, 223−230.

(3) Henzler-Wildman, K., and Kern, D. (2007) Dynamic personalities of proteins. *Nature 450*, 964−972.

(4) Lang, P. T., Ng, H.-L., Fraser, J. S., Corn, J. E., Echols, N., Sales, M., Holton, J. M., and Alber, T. (2010) Automated electron-density sampling reveals widespread conformation polymorphism in proteins. *Protein Sci. 19*, 1420−1431.

(5) Eisenmesser, E. Z., Millet, O., Labeikovsky, W., Korzhnev, D. M., Wolf-Watz, M., Bosco, D. A., Skalicky, J. J., Kay, L. E., and Kern, D. (2005) Intrinsic dynamics of an enzyme underlies catalysis. *Nature 438*, 117−121.

(6) Fraser, J. S., Clarkson, M. W., Degnan, S. C., Erion, R., Kern, D., and Alber, T. (2009) Hidden alternative structures of proline isomerase essential for catalysis. *Nature 462*, 669−673.

(7) Bouvignies, G., Vallurupalli, P., Hansen, D. F., Correia, B. E., Lange, O., Bah, A., Vernon, R. M., Dahlquist, F. W., Baker, D., and Kay, L. E. (2011) Solution structure of a minor and transiently formed state of a T4 lysozyme mutant. *Nature 477*, 111−114.

(8) Henzler-Wildman, K. A., Thai, V., Lei, M., Ott, M., Wolf-Watz, M., Fenn, T., Pozharski, E., Wilson, M. A., Petsko, G. A., Karplus, M., Huebner, C. G., and Kern, D. (2007) Intrinsic motions along an enzymatic reaction trajectory. *Nature 450*, 838−844.

(9) Wilson, M. T., and Greenwood, C. (1996) The alkaline transition in ferricytochrome *c*. In *Cytochrome c: A Multidisciplinary Approach* (Scott, R. A., and Mauk, A. G., Eds.) pp 611−634, University Science Books, Sausalito, CA.

(10) Cherney, M. M., and Bowler, B. E. (2011) Protein dynamics and function: Making new strides with an old warhorse, the alkaline conformational transition of cytochrome *c*. *Coord. Chem. Rev. 255*, 664−677.

(11) Rosell, F. I., Ferrer, J. C., and Mauk, A. G. (1998) Proton-linked protein conformational switching: Definition of the alkaline conformational transition of yeast iso-1-ferricytochrome *c*. *J. Am. Chem. Soc. 120*, 11234−11245.

(12) Assfalg, M., Bertini, I., Dolfi, A., Turano, P., Mauk, A. G., Rosell, F. I., and Gray, H. B. (2003) Structural model for an alkaline form of ferricytochrome *c*. *J. Am. Chem. Soc. 125*, 2913−2922.

(13) Kristinsson, R., and Bowler, B. E. (2005) Communication of stabilizing energy between substructures of a protein. *Biochemistry 44*, 2349−2359.

(14) Nelson, C. J., and Bowler, B. E. (2000) pH dependence of formation of a partially unfolded state of a Lys 73 → His variant of iso-1-cytochrome *c*: Implications for the alkaline conformational transition of cytochrome *c*. *Biochemistry 39*, 13584−13594.

(15) Ow, Y. P., Green, D. R., Hao, Z., and Mak, T. W. (2008) Cytochrome *c*: Functions beyond respiration. *Nat. Rev. Mol. Cell Biol. 9*, 532−542.

(16) Yu, T., Wang, X., Purring-Koch, C., Wei, Y., and McLendon, G. L. (2001) A mutational epitope for cytochrome *c* binding to the apoptosis protease activation factor-1. *J. Biol. Chem. 276*, 13034−13038.

(17) Olteanu, A., Patel, C. N., Dedmon, M. M., Kennedy, S., Linhoff, M. W., Minder, C. M., Potts, P. R., Deshmukh, M., and Pielak, G. J. (2003) Stability and apoptotic activity of recombinant human cytochrome *c*. *Biochem. Biophys. Res. Commun. 312*, 733−740.

(18) Kluck, R. M., Martin, S. J., Hoffman, B. M., Zhou, J. S., Green, D. R., and Newmeyer, D. D. (1997) Cytochrome *c* activation of CPP32-like proteolysis plays a critical role in a *Xenopus* cell-free apoptosis system. *EMBO J. 16*, 4639−4649.

(19) Ellerby, H. M., Martin, S. J., Ellerby, L. M., Naiem, S. S., Rabizadeh, S., Salvesen, G. S., Casiano, C. A., Cashman, N. R., Green, D. R., and Bredesen, D. E. (1997) Establishment of a cell-free system of neuronal apoptosis: Comparison of premitochondrial, mitochondrial, and postmitochondrial phases. *J. Neurosci. 17*, 6165−6178.

(20) Kluck, R. M., Ellerby, L. M., Ellerby, H. M., Naiem, S., Yaffe, M. P., Margoliash, E., Bredesen, D., Mauk, A. G., Sherman, F., and Newmeyer, D. D. (2000) Determinants of cytochrome *c* pro-apoptotic activity. The role of lysine 72 trimethylation. *J. Biol. Chem. 275*, 16127−16133.

(21) Kagan, V. E., Tyurin, V. A., Jiang, J., Tyurina, Y. Y., Ritov, V. B., Amoscato, A. A., Osipov, A. N., Belikova, N. A., Kapralov, A. A., Kini, V., Vlasova, I. I., Zhao, Q., Zou, M., Di, P., Svistunenko, D. A., Kurnikov, I. V., and Borisenko, G. G. (2005) Cytochrome *c* acts as a cardiolipin oxygenase required for release of proapoptotic factors. *Nat. Chem. Biol. 1*, 223−232.

(22) Kapetanaki, S. M., Silkstone, G., Husu, I., Liebl, U., Wilson, M. T., and Vos, M. H. (2009) Interaction of carbon monoxide with the apoptosis-inducing cytochrome *c*-cardiolipin complex. *Biochemistry 48*, 1613−1619.

(23) Silkstone, G., Kapetanaki, S. M., Husu, I., Vos, M. H., and Wilson, M. T. (2012) Nitric oxide binding to the cardiolipin complex of ferric cytochrome *c*. *Biochemistry 51*, 6760−6766.

(24) Bradley, J. M., Silkstone, G., Wilson, M. T., Cheesman, M. R., and Butt, J. N. (2011) Probing a complex of cytochrome *c* and cardiolipin by magnetic circular dichroism spectroscopy: Implications for the initial events in apoptosis. *J. Am. Chem. Soc. 133*, 19676−19679.

(25) Jemmerson, R., Liu, J., Hausauer, D., Lam, K. P., Mondino, A., and Nelson, R. D. (1999) A conformational change in cytochrome *c* of apoptotic and necrotic cells is detected by monoclonal antibody binding and mimicked by association of the native antigen with synthetic phospholipid vesicles. *Biochemistry 38*, 3599−3609.

(26) Diederix, R. E. M., Ubbink, M., and Canters, G. W. (2002) Peroxidase activity as a tool for studying the folding of c-type cytochromes. *Biochemistry 41*, 13067−13077.

(27) Berghuis, A. M., and Brayer, G. D. (1992) Oxidation state-dependent conformational changes in cytochrome *c*. *J. Mol. Biol. 223*, 959−976.

(28) Pollock, W. B., Rosell, F. I., Twitchett, M. B., Dumont, M. E., and Mauk, A. G. (1998) Bacterial expression of a mitochondrial cytochrome *c*. Trimethylation of Lys72 in yeast iso-1-cytochrome *c* and the alkaline conformational transition. *Biochemistry 37*, 6124−6131.

(29) Bandi, S., Baddam, S., and Bowler, B. E. (2007) Alkaline conformational transition and gated electron transfer with a Lys 79 → His variant of iso-1-cytochrome *c*. *Biochemistry 46*, 10643−10654.

(30) Duncan, M. G., Williams, M. D., and Bowler, B. E. (2009) Compressing the free energy range of substructure stabilities in iso-1-cytochrome *c*. *Protein Sci. 18*, 1155−1164.

(31) Rosell, F. I., and Mauk, A. G. (2002) Spectroscopic properties of a mitochondrial cytochrome *c* with a single thioether bond to the heme prosthetic group. *Biochemistry 41*, 7811−7818.

(32) Rumbley, J. N., Hoang, L., and Englander, S. W. (2002) Recombinant equine cytochrome *c* in *Escherichia coli*: High-level expression, characterization, and folding and assembly mutants. *Biochemistry 41*, 13894−13901.

(33) Kurchan, E., Roder, H., and Bowler, B. E. (2005) Kinetics of loop formation and breakage in the denatured state of iso-1-cytochrome *c*. *J. Mol. Biol. 353*, 730−743.

(34) Wandschneider, E., Hammack, B. N., and Bowler, B. E. (2003) Evaluation of cooperative interactions between substructures of iso-1-cytochrome *c* using double mutant cycles. *Biochemistry 42*, 10659−10666.
(35) Redzic, J. S., and Bowler, B. E. (2005) Role of hydrogen bond networks and dynamics in positive and negative cooperative stabilization of a protein. *Biochemistry 44*, 2900−2908.
(36) Santoro, M. M., and Bolen, D. W. (1992) A test of the linear extrapolation of unfolding free energy changes over an extended denaturant concentration range. *Biochemistry 31*, 4901−4907.
(37) Hagihara, Y., Tan, Y., and Goto, Y. (1994) Comparison of the conformational stability of the molten globule and native states of horse cytochrome *c*. *J. Mol. Biol. 237*, 336−348.
(38) Godbole, S., Hammack, B., and Bowler, B. E. (2000) Measuring denatured state energetics: Deviations from random coil behavior and implications for the folding of iso-1-cytochrome *c*. *J. Mol. Biol. 296*, 217−228.
(39) Moore, G. R., and Pettigrew, G. W. (1990) *Cytochromes c: Evolutionary, Structural and Physicochemical Aspects*, Springer-Verlag, New York.
(40) Baddam, S., and Bowler, B. E. (2005) Thermodynamics and kinetics of formation of the alkaline state of a Lys 79→Ala/Lys 73→His variant of iso-1-cytochrome *c*. *Biochemistry 44*, 14956−14968.
(41) Margoliash, E., and Frohwirt, N. (1959) Spectrum of horse-heart cytochrome *c*. *Biochem. J. 71*, 570−572.
(42) Battistuzzi, G., Borsari, M., De Rienzo, F., Di Rocco, G., Ranieri, A., and Sola, M. (2007) Free energy of transition for the individual alkaline conformers of yeast iso-1-cytochrome c. *Biochemistry 46*, 1694−1702.
(43) Hammack, B. N., Smith, C. R., and Bowler, B. E. (2001) Denatured state thermodynamics: Residual structure, chain stiffness and scaling factors. *J. Mol. Biol. 311*, 1091−1104.
(44) Betz, S. F., and Pielak, G. J. (1992) Introduction of a disulfide bond into cytochrome *c* stabilizes a compact denatured state. *Biochemistry 31*, 12337−12344.
(45) Myers, J. K., Pace, C. N., and Scholtz, J. M. (1995) Denaturant *m* values and heat capacity changes: Relation to changes in accessible surface areas of protein unfolding. *Protein Sci. 4*, 2138−2148.
(46) Bandi, S., and Bowler, B. E. (2013) A cytochrome *c* electron transfer switch modulated by heme ligation and isomerization of a peptidyl-prolyl bond. *Biopolymers*, DOI: 10.1002/bip.22164.
(47) Bandi, S., and Bowler, B. E. (2011) Probing the dynamics of a His73-heme alkaline conformer in a destabilized variant of yeast iso-1-cytochrome *c* with conformationally gated electron transfer methods. *Biochemistry 50*, 10027−10040.
(48) Bandi, S., and Bowler, B. E. (2008) Probing the bottom of a folding funnel using conformationally gated electron transfer reactions. *J. Am. Chem. Soc. 130*, 7540−7541.
(49) Baddam, S., and Bowler, B. E. (2006) Tuning the rate and pH accessibility of a conformational electron transfer gate. *Inorg. Chem. 45*, 6338−6346.
(50) Baddam, S., and Bowler, B. E. (2005) Conformationally gated electron transfer in iso-1-cytochrome *c*: Engineering the rate of a conformational switch. *J. Am. Chem. Soc. 127*, 9702−9703.
(51) Martinez, R. E., and Bowler, B. E. (2004) Proton-mediated dynamics of the alkaline conformational transition of yeast iso-1-cytochrome *c*. *J. Am. Chem. Soc. 126*, 6751−6758.
(52) Nelson, C. J., LaConte, M. J., and Bowler, B. E. (2001) Direct detection of heat and cold denaturation for partial unfolding of a protein. *J. Am. Chem. Soc. 123*, 7453−7454.
(53) Godbole, S., and Bowler, B. E. (1999) Effect of pH on formation of a nativelike intermediate on the unfolding pathway of a Lys 73 → His variant of yeast iso-1-cytochrome *c*. *Biochemistry 38*, 487−495.
(54) Godbole, S., Dong, A., Garbin, K., and Bowler, B. E. (1997) A lysine 73 → histidine variant of yeast iso-1-cytochrome *c*: Evidence for a native-like intermediate in the unfolding pathway and implications for *m* value effects. *Biochemistry 36*, 119−126.
(55) Davis, L. A., Schejter, A., and Hess, G. P. (1974) Alkaline isomerization of oxidized cytochrome *c*. Equilibrium and kinetic measurements. *J. Biol. Chem. 249*, 2624−2632.
(56) Baddam, S., and Bowler, B. E. (2006) Mutation of asparagine 52 to glycine promotes the alkaline form of iso-1-cytochrome *c* and causes loss of cooperativity in acid unfolding. *Biochemistry 45*, 4611−4619.
(57) Myer, Y. P., MacDonald, L. H., Verma, B. C., and Pande, A. (1980) Urea denaturation of horse heart ferricytochrome *c*. Equilibrium studies and characterization of intermediate forms. *Biochemistry 19*, 199−207.
(58) Angström, J., Moore, G. R., and Williams, R. J. P. (1982) The magnetic-susceptibility of ferricytochrome *c*. *Biochim. Biophys. Acta 703*, 87−94.
(59) Shah, R., and Schweitzer-Stenner, R. (2008) Structural changes of horse heart ferricytochrome *c* induced by changes of ionic strength and anion binding. *Biochemistry 47*, 5250−5257.
(60) Hagarman, A., Duitch, L., and Schweitzer-Stenner, R. (2008) The conformational manifold of ferricytochrome *c* explored by visible and far-UV electronic circular dichroism spectroscopy. *Biochemistry 47*, 9667−9677.
(61) Robinson, M. N., Boswell, A. P., Huang, Z.-X., Eley, C. G. S., and Moore, G. R. (1983) The conformation of eukaryotic cytochrome *c* around residues 39, 57, 59 and 74. *Biochem. J. 213*, 687−700.
(62) Weinkam, P., Zimmermann, J., Sagle, L. B., Matsuda, S., Dawson, P. E., Wolynes, P. G., and Romesberg, F. E. (2008) Characterization of alkaline transitions in ferricytochrome *c* using carbon-deuterium infrared probes. *Biochemistry 47*, 13470−13480.
(63) Verbaro, D., Hagarman, A., Soffer, J., and Schweitzer-Stenner, R. (2009) The pH dependence of the 695 nm charge transfer band reveals the population of an intermediate state of the alkaline transition of ferricytochrome *c* at low ion concentrations. *Biochemistry 48*, 2990−2996.
(64) Sanchez, R., and Zhou, M.-M. (2011) The PHD finger: A versatile epigenomic reader. *Trends Biochem. Sci. 36*, 364−372.
(65) Daze, K. D., and Hof, F. (2013) The cation-π interaction at protein-protein interaction interfaces: Developing and learning from synthetic mimics of protein that bind methylated lysines. *Acc. Chem. Res.*, DOI: 10.1021/ar300072g.